

A novel mechatronic system for measuring end-point stiffness

Mechanical design and preliminary tests

L. Masia¹, G. Sandini¹ and P.G. Morasso¹

Italian Institute of Technology, Robotics Brain and Cognitive Sciences Dept.
Genoa, Italy

lorenzo.masia@iit.it; giulio.sandini@iit.it; pietro.morasso@iit.it

Abstract— Measuring arm stiffness is of great interest for many disciplines from biomechanics to medicine especially because modulation of impedance represents one of the main mechanism underlying control of movement and interaction with external environment. Previous works have proposed different methods to identify multijoint hand stiffness by using planar or even tridimensional haptic devices, but the associated computational burden makes them not easy to implement. We present a novel mechanism conceived for measuring multijoint planar stiffness by a single measurement and in a reduced execution time. A novel mechanical rotary device applies cyclic radial perturbation to human arm of a known displacement and the force is acquired by means of a 6-axes commercial load cell. The outcomes suggest that the system is not only reliable but allows obtaining a bi-dimensional estimation of arm stiffness in reduced amount of time and the results are comparable with those reported in previous researches.

Keywords— component; hand stiffness; rotary mechanism; mechatronic device.

I. INTRODUCTION

The mechanical impedance of a dynamic system is a physical characteristic defining the reactive force of the system itself in response to an imposed spatial perturbation. Mechanical impedance of neuromuscular system can be seen as the contribution of three different terms: stiffness, viscosity and inertia. Hand mechanical impedance is of particular interest for understanding the control strategy underlying the interaction with external environment and its modulation during movement is a fundamental factor in the study of the biological approach in preservation of stability during manipulation task [1]. In multijoint arm movements endpoint impedance of the arm is the result of the interaction between agonist and antagonist muscles concurrent on a joint which are characterized by an inherently spring-like properties [2]. Most of the previous works focused the attention to the stiffness measurement, because contrarily to viscoelastic and inertial contributions, stiffness is directly modulated by the central nervous system (CNS) by changing the activation levels of agonist and antagonist muscles. The widely used technique for stiffness evaluation is based on the acquisition of muscular restoring force resulting to a known displacement. The seminal work of Mussa-Ivaldi et al. [3] proposed a new experimental method using computer controlled mechanical interface to measure and represent the elastic force field associated to the posture of the arm; it consisted in observing

the steady-state force responses to a series of separate one-dimensional 'step' perturbations imposed from different directions; it was found that the endpoint stiffness of the human arm in the horizontal plane was primarily 'spring-like' and that limb geometry had a major effect on the magnitude and directionality of endpoint stiffness. Several other studies have used similar techniques to examine the effects of external loads. Bennet et al. [4-5] and Lacquaniti et al. [6] have used stochastic force disturbance and consequently measuring the resulting change in hand position. Robot generated force impulses have been used to estimate stiffness during multijoint movements [7-11] and a further experimental investigation by Burdet et al. [12] strengthen the robustness of this technique by introducing an algorithm allowing to modulate the hand displacement relative to a prediction of the unperturbed trajectory.

A time-domain and frequency domain, multiple-input, multiple-output (MIMO) linear system identification techniques was also adopted to estimate the dynamic endpoint stiffness of a multijoint limb [13]. This last model was proposed in order to overcome the limitations showed by the previous mentioned method based on the step-perturbation. In fact estimates of steady-state stiffness, obtained using step or ramp perturbations, require that the subjects 'do not intervene' in response to step or pulse changes in end-point position for intervals several times longer than stretch reflex or even voluntary reaction times. Besides the steady-state stiffness estimates, employed in most studies, ignore the much larger dynamic stiffness components that can strongly resist transient external disturbances; again the examination of the dynamic endpoint properties (inertia, viscoelasticity) was performed with a priori assumptions about the structure of the endpoint dynamics based on a second order linear model.

Despite all these efforts, endpoint impedance measurement still remains hard to implement and variability of the conditions may lead to high inaccuracy and reliability of data. Recent researches were focused on the development of mechatronic devices characterized by low impedance at the end effector and therefore high backdriveability [14-15-16]: all these systems were actually planar 2D manipulanda used to perturb human arm (shoulder and elbow) in different directions using impedance or force control schemes and consequently sensing the restoring force at the interaction between the device and the human arm. The theoretical

approaches for data post processing for impedance evaluation were the ones above mentioned.

We propose a novel mechanism designed for impedance evaluation based on a modular device coupled with a commercial force sensor which can be applied at the end effector of any robotic manipulandum; characterized by an extremely high bandwidth and able to measure endpoint impedance in multiple directions in an extremely short time (less than 1 second) and it doesn't need for any implementation of complex control scheme to apply kinematic perturbations.

II. MECHANICAL DESIGN

The system can be described by dividing the whole assembly in two main parts:

- **measuring module:** it consists of a commercial six-axes force sensor (ATI Gamma, ATI Industrial Automation, NC, USA).
- **motion generator:** the motion generator is a novel mechanism which superimpose the motion pattern to the force sensor and therefore it represents the module which applies the series of separate one-directional 'step' perturbations imposed from different directions.

The **motion generator** is made by a planetary gear with its **sun-gear** coupled to a main shaft rigidly connected to a minimum jerk profiled **cam** (figure 1). The **sun** is driven by the primary actuator which transmits the motion to the whole system and it is a brushless torque controlled electric motor.

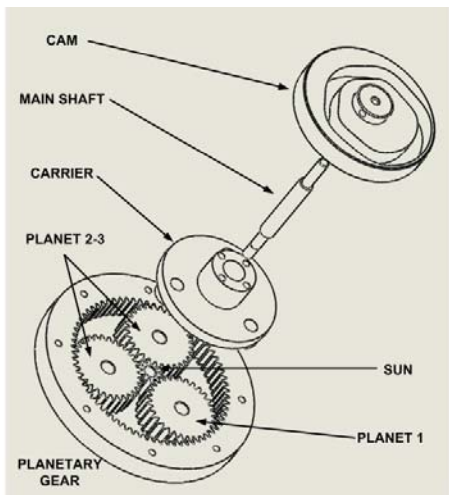


Figure 1: motion-generator is the assembly of a planetary gearhead and a cam mounted on the main shaft which delivers the motion.

The system is designed to have a theoretical reduction ratio of 8:1; this means that 8 rounds of the **cam** and the **sun** correspond to 1 complete rotation of **carrier** which is connected to the three **planets** of the planetary gearhead. The **carrier** is equipped with linear bearings which can slide in the horizontal plane with a motion law superimposed by the cam profile. The above mentioned steady-state force responses method using directional perturbation requires that there be an

interval during which the hand is maintained in a zero velocity position after being displaced and this interval is indicated as a plateau (figure 2). As suggested by Burdet et al. [17] in order to have a good estimation of the stiffness using steady state displacement a good position perturbation must be brief, and the constant position plateau (dwell in which the force is measured) must be reached as quickly as possible.

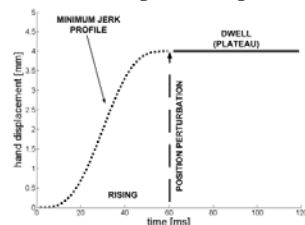


Figure 2: typical 4mm perturbation superimposed to end point in order to measure the restoring force during the plateau at which the inertial contribution of the arm is negligible.

However, a too fast or abrupt transition to the plateau requires the mechanical interface to produce high forces within a brief time, which can lead to vibration and deterioration of the force signal. A short transition phase, which minimized vibration, was achieved by designing the **cam** profile using a sixth-order polynomial with zero velocity and zero acceleration at the boundaries and zero end jerk according the following formula [18]:

$$x(\theta) = C_0 + C_1x + \dots + C_5x^5 + C_6x^6 \quad (1)$$

Where $x(\theta)$ is the imposed displacement of the **cam** as function of the **cam** rotation and $C_{0..6}$ are the unknown coefficients of the 6th order polynomial to be determined to match the design specification of jerk minimization. It was chosen to use a double dwell **cam** which, in 360 degrees rotation, displaces the subject's hand in two different opposite directions to input an "unpredictable" perturbation (figure 3).

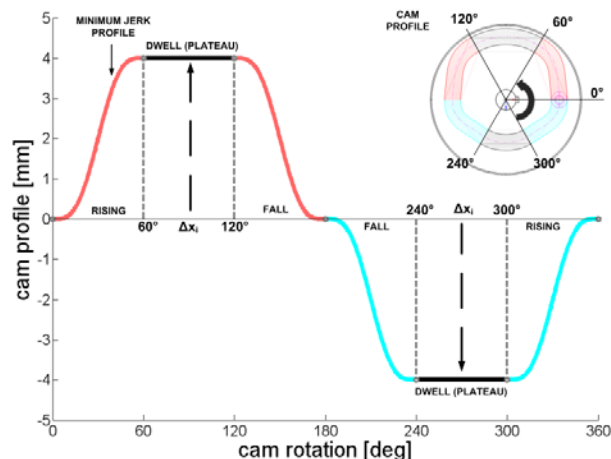


Figure 3: cam profile obtained by a sixth order polynomial allows a 4mm displacement by a double dwell minimizing the acceleration and jerk while risings.

The main purpose of the **motion module** is perturbing the end point in different radial directions; as previously mentioned the **carrier** is equipped with linear bearings on which the force sensor is mounted (figure 4) and therefore every rotation of the **carrier** the **cam** radially moves the force sensor in **sixteen** (the

cam is *double dwell* for *eight* rounds the *cam profile* perturbs 8x2 times) different directions (the theoretical reduction ratio is 8:1). For clarity sake of the sketch in figure 4 only 8 direction are depicted.

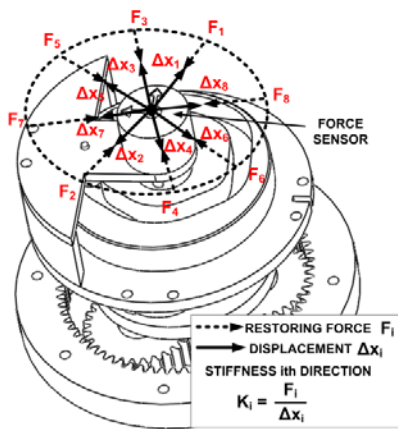


Figure 4: mechanical sketch of the assembly and radial perturbations: on the top the force sensor is rigidly connected to the end effector and superimposes different radial perturbation ΔX_i due to cam rotation over the course of planetary gear motion. Only 8 directions are depicted to simplify the sketch.

Once the system starts (figure 4) the *cam* pushes the *sliding carriage* and the *force sensor* in one direction, displacing the *subject's hand* of a certain amount ΔX_1 that is defined by the geometry of the *cam profile*. The *hand force* reaction F_1 is acquired by the *force sensor*, hence a directional value of the stiffness K_1 is obtained as the ratio:

$$K_1 = \frac{F_1}{\Delta X_1}$$

While the *cam* rotates, the *carrier* and the *sliding carriage* rotate with a slower angular speed, which is imposed by the *reduction ratio* of the *planetary gear head* (8:1). The next half round of the *cam* perturbs the *hand* in an opposed direction shifted with respect to the previous one of the amount of rotation made by the *carrier* and 180° because the *cam* is double-dwell. The hand is now displaced of a ΔX_2 and the correspondent reaction force F_2 is acquired by means of the *force sensor*. The stiffness associated to the new direction will be:

$$K_2 = \frac{F_2}{\Delta X_2}$$

Since directional arm stiffness is not isotropic but strongly depends on muscular activation and posture the two evaluated stiffness K_1 and K_2 are different.

When the *planetary gearhead* or the *carrier* completes one round, the system will have scanned *sixteen* (*eight X 2*) different directions, because 8:1 is the reduction ratio of the *planetary gear* and sixteen values of directional stiffness will have been evaluated.

$$K_1 = \frac{F_1}{\Delta X_1}; K_2 = \frac{F_2}{\Delta X_2}; K_3 = \frac{F_3}{\Delta X_3} \dots K_k = \frac{F_k}{\Delta X_k}; \dots K_8 = \frac{F_8}{\Delta X_8}$$

Using such designed system it is possible to estimate multidirectional stiffness in a very short time and therefore there is no need to perform numerous distinct trials for different directional measurements as suggested by the steady-state force responses method.

III. METHODS AND EXPERIMENTS

A. Characterization of the system: preliminary test.

Measuring hand stiffness is not a trivial task; previous methods suffer from the limitation that a perturbation of the same amplitude, during different trajectories, applied at different points in the trajectory or in different directions, will displace the hand by different amounts. This is because limb stiffness depends on joint angles, angular velocity and perturbation direction; hence the proposed mechanical device has the main goal to allow measuring stiffness without disrupting motion concentrating the acquisition in only one trajectory. Before testing the device on humans to characterize the system a custom setup has been developed (figure 5). It consists of a bench where the device is connected to a frame able simulate different stiffness configurations by means of calibrated springs. Multiple stiffness configurations at distinct speeds of the mechanism have been measured to test the accuracy and reliability of the device. It is important to precise that simulating an accurate stiffness value is almost impossible but a preferential stiffness orientation can be simulated by disposing the springs in a certain configuration. The measures will be then focused on the capability of the device to accurately identify the orientation of the stiffness ellipse and not its absolute value.

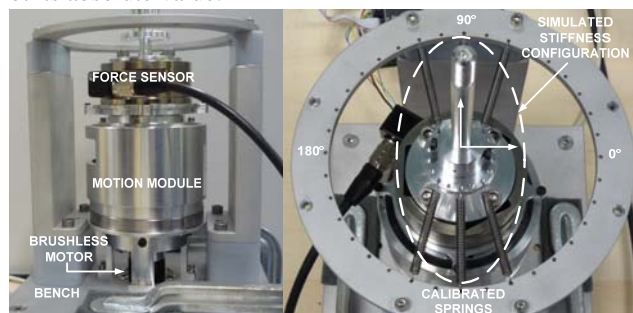


Figure 5: overview of the device (motion module and force sensors) connected to the bench used to simulate principal direction of stiffness by calibrated springs.

Table I indicates the speed values at which the system performs the stiffness measurement for the chosen configuration of the calibrated springs disposed on the bench and connected to the force sensor.

Table I: experimental condition of the preliminary test

Rpm	100	300	500	800	1000	1200	1500	2000
Execution time [s]	13.47	4.49	2.69	1.83	1.45	1.24	0.96	0.75
Principal direction	90° on the plane XY of the force sensor							

Looking at the plot depicting the absolute value of the force during the *carrier* rotation, we can observe that the *cam* does not rotate the expected value by the theoretical reduction ratio

8:1. In fact one could expect that in 180° of rotation (half round was chosen in order to limit the time of execution) of the *carrier* the *cam* should have rotated four times, but the reduction ratio of the planetary gearhead was lower than the theoretical one; this is mainly due to systematic manufacturing inaccuracy in gears machining. Observing figure 6 it is possible to identify the force peaks corresponding to the 4mm dwells of the *cam* (2 dwells each rotation) which are not eight as expected but seven.

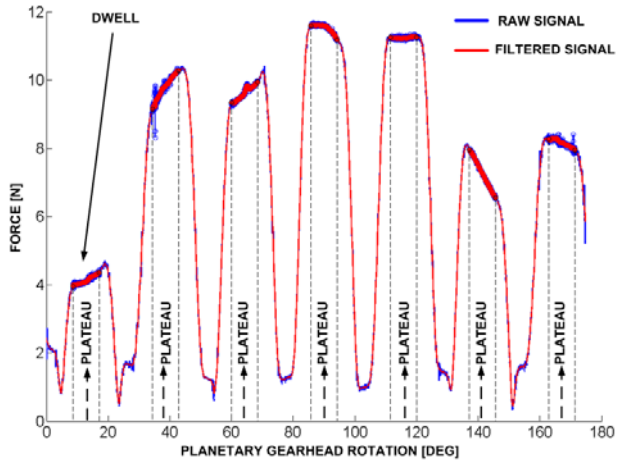


Figure 6: plot of the force during cam dwells in function of the angular rotation of the planetary gearhead. The blue trace corresponds to the raw value of the absolute force while the red one is filtered by a second order Butterworth filter (cutoff frequency 10 Hz).

A second order Butterworth filter (10 Hz cut-off frequency) was used to clean the force signal from oscillations and noise during the acquisition. The intervals of interest for measuring the stiffness over the seven directions are the dwells of the *cam* where the springs are stretched by 4mm displacements and are indicated in figure 6 as *plateaus*. In this phase the amount of restoring force is acquired and divided by the actual displacement (4mm) imposed by the rotation of the *cam profile* in order to obtain every single directional stiffness which is then associated to the planetary gearhead rotation interval in which displacement is given.

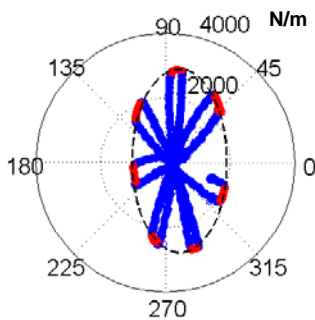


Figure 7: visualization of planar stiffness measurement over the different directions of perturbation executed in one single trial.

Figure 7 depicts the two-dimensional stiffness calculated using the previous described method. It is clear observing the configuration of the calibrated springs from figure 6 that the direction of higher stiffness corresponds to 90 and 270 degrees approximately. The dotted black ellipse is a fitting performed by nonlinear least squares, optimizing the squared sum of

orthogonal distances from the points to the fitted ellipse. Observing figure 7 it is evident that the centre of the ellipse is shifted rightward; this is not due to inaccuracy or drift in the measurement but to the tolerances in mounting procedure because the centre of the force sensor and the one of the frame on which the device is mounted may not be coincident. In order to perform measurement on humans, it is crucial to obtain at the minimum time execution at which the device can measure two-dimensional stiffness. Past works referred to an 8-10 mm single directional perturbation of 300 ms duration; in our method the device must space 7 different directions in the shortest time as possible maintaining an acceptable level of accuracy and repeatability.

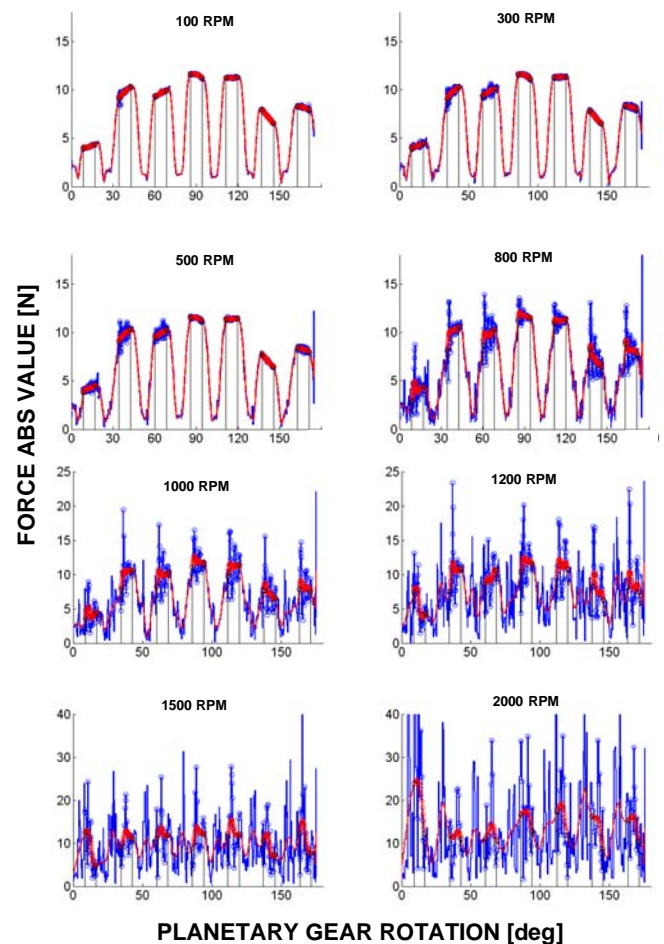


Figure 8: force signals raw (blue) and filtered (red) for different trials at different angular speed of the mechanism. As clearly shown from increasing the angular speed a vibrational noise emerges affecting the measurement.

Figure 8 depicts to the absolute value of the force as function of angular rotation of the *carrier* and the *planetary gear* during the trials at different angular speeds of the *cam*. As shown in the plots, for high angular speeds (800-1200-1500-2000 RPM) despite filtering the force signal is affected by mechanical noise especially in correspondence to the *dwells* of the *cam*, where a second order oscillation arises because of an increasing contribution of inertial counterpart of the mechanics. The resulting stiffness calculation will be more or less accurate depending on the efficacy of data filtering, in fact from figure 9

emerges that the two-dimensional stiffness measurements are not acceptable for rotational regimes up to 1200 RPM; at this high speed despite the data (red points) result more spread out, the interpolating ellipse preserves a shape comparable with those for obtained at lower speeds, whereas for higher value (1500-2000 RPM) the stiffness calculation is dramatically jeopardized by mechanical noise.

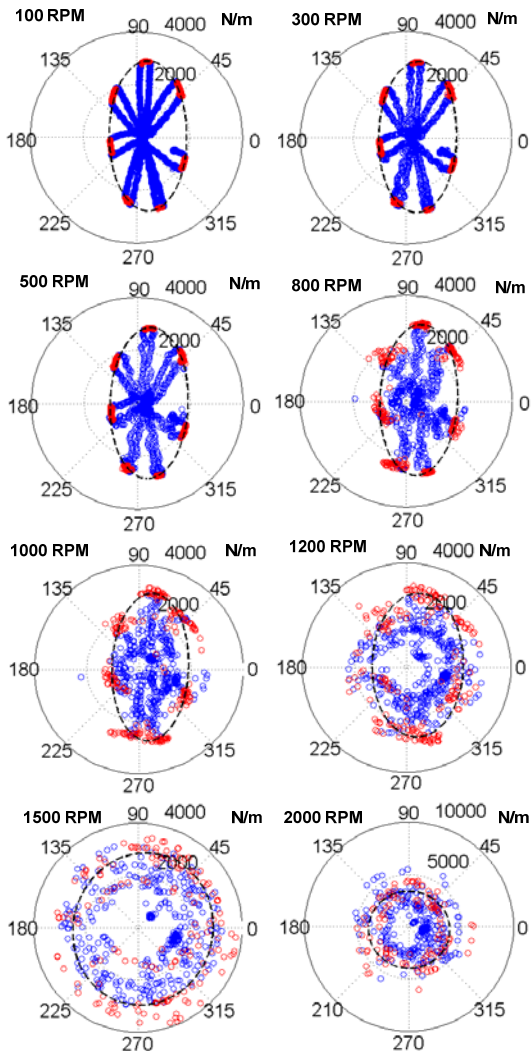


Figure 9: visualization of the estimated stiffness at different speeds.

It is important to point that the above described test has been performed using a mechanical setup with springs and no damper or absorbing elements which could limit vibrations; contrarily the device was conceived and developed for experiments on humans, where biological tissues result in different stiffness than the one simulated by the previous setup and muscular viscosity plays a considerable counterpart in limiting or even extinguishing any vibrational phenomenon.

B. Preliminary test on human.

We tested the system on a human subject; this is a very preliminary test where endpoint stiffness was estimated using the device; one subject took a seat in front of the device and his right shoulder was restrained by a seatbelt; he was

instructed to grasp the handle of the device and stiff the arm at maximum voluntary contraction (MVC) (figure 10); before performing the test the subject was instructed to stiff the arm trying not to apply force in a preferred direction but holding the hand in position and a visual feedback was provided showing the direction of the applied force. Five different trials were recorded for three different arm postures at 1500 RPM of the mechanism.

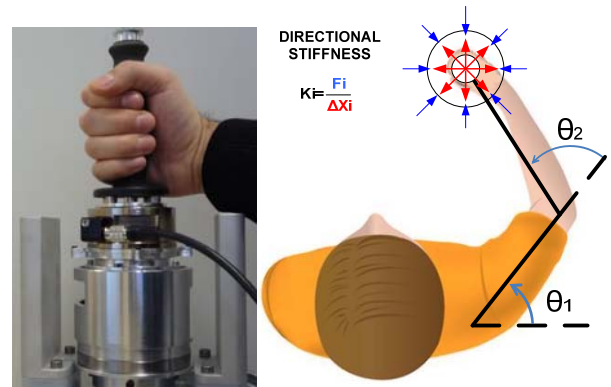
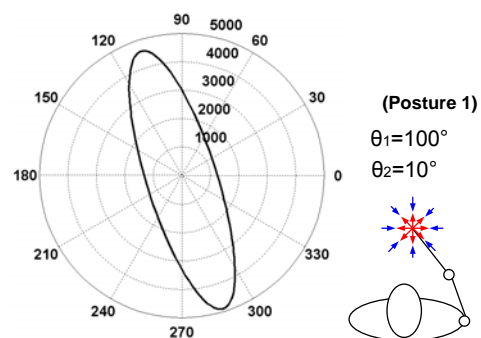


Figure 10: device equipped with handle for human trials.

Results are shown in figure 11 where each interpolating ellipse is obtained from the 5 trials for each posture of the arm which is indicated in the bottom by a sketch; three different arm configurations were chosen in order to highlight the difference in stiffness ellipse orientation when subject is required to perform MVC holding position task. As shown in the polar plots the ellipses are positioned at a location proportional to the force magnitude and biased in the direction the subject was exerting the force during MVC. As expected the direction of the major axes of the ellipse changes as function of arm configuration; the major axis of the ellipses becomes more elongated as the hand location is moved in a more distal position (figure 11.1-2), while it is more isotropic as the hand location is closer to a proximal configuration (figure 11.3). The value of the stiffness resulted very large, but this is likely consistent with the adopted methodology of the experiment in which a MVC was requested to start the acquisition; using maximum voluntary contraction was fundamental to increase the contact between the handle of the device and the hand of the subject during the directional displacement superimposed by the mechanism, but in the future a rigid set up constraining the wrist will be adopted.



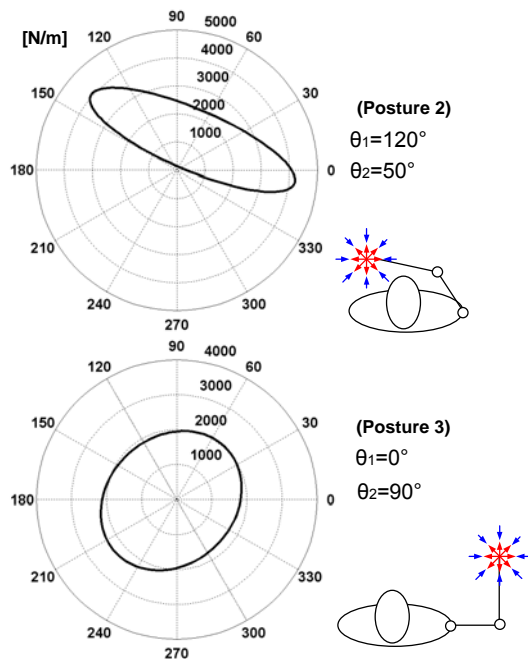


Figure 11: preliminary results on a human subject; the black ellipse are obtained by interpolating 5 different trials for each posture.

IV. DISCUSSION

This work proposes a novel device to measure planar endpoint stiffness. The past literature was mainly focused on suggesting multiple methodological approaches for observation of multi-joint characteristics (stiffness, inertia and viscosity) and of course they still represent a valid and robust method to investigated neural mechanism underlying control of movement and impedance modulation. Nevertheless nobody has concentrated efforts on designing hardware and sensors in order to decrease the computational burden and the theoretical assumptions beyond impedance measurement. It is worth to notice that almost all of the studies on stiffness evaluation were performed using planar manipulanda; such systems on one side are highly backdriveable and accurate in position and force measurement but, on the other side, have limited position bandwidth due to their mass and motor inertia that must satisfy specific requirements for the haptic rendering. The need of having a modular system that can be mounted on the end-effector of such planar systems, and completely uncoupled from the implementation of control schemes driving the robot, may be a valid alternative for studying arm characteristic while manipulation tasks. The present paper highlighted the difficulties and the limits underlying the design of such kind of device: a fast multidirectional measurement leads to vibrations and noise that may affect the measure. Despite all we think that improvements in the system design can lead to much more accurate and reliable experimental results. We decided to focus the measurement on the stiffness counterpart of the arm impedance but a new mechanical design refinement is already ongoing and will allow estimating all the components of muscular activity. The main idea is using the method proposed by Perrault et al. [13] consisting on stochastic perturbation to estimate impedance in a very short time (less than 0.5 s) using the proposed device mounted on our planar manipulandum

[19]. This method is in contrast to the standard steady-state methodology discussed in the introduction of the present work, that requires different trials (trajectories in a reaching task) to measure impedance with the additional uncertainty associated to trial-to-trial variability in subjects' performance. Besides estimation of impedance by using steady-state method requires that the subject does not intervene when the step perturbation is superimposed, and it is difficult to detect voluntary reactions which may strongly affect the measures. Due to the design and simplicity of the proposed device (1DoF) our purpose is succeed in generating a stochastic unpredictable perturbation in a time short enough to anticipate the voluntary reaction. Once the system is mounted on a planar manipulandum hopefully it will be possible to study force field adaptation paradigms and at the same time without any additional algorithm to use the device in order to obtain a real time reading of the impedance modulation while performing different tasks in simulated environments.

ACKNOWLEDGMENT

This work was carried out at Motor Learning and Rehabilitation Laboratory of Italian Institute of Technology and it was supported by a grant of Italian Ministry of Scientific Research and Ministry of Economy. This work is partly supported by the EU grant FP7- ICT-271724 HUMOUR and FP7-ICT-2007-3 VIATORS.

REFERENCES

- [1] Hogan, N., 1985. The mechanics of multi-joint posture and movement control. *Biological Cybernetics* 52, 315-331.
- [2] Feldman AG (1966) Functional tuning of nervous system with control of movement or maintenance of a steady posture. III. Mechanographic analysis of the execution by man of the simplest motor tasks. *Biofizika* 11:667-675.
- [3] Mussa-Ivaldi, F.A., Hogan, N., Bizzi, E., 1985. Neural, mechanical, and geometric factors subserving arm posture in humans. *Journal of Neuroscience* 5, 2732-2743.
- [4] Bennett, D.J., 1993. Torques generated at the human elbow joint in response to constant position errors imposed during voluntary movements. *Experimental Brain Research* 95, 488-498.
- [5] Bennett, D.J., Hollerbach, J.M., Xu, Y., Hunter, I.W., 1992. Timevarying stiffness of human elbow joint during cyclic voluntary movement. *Experimental Brain Research* 88, 433-442.
- [6] Lacquaniti, F., Carrozzo, M., Borghese, N.A., 1993. Time-varying mechanical behavior of multijointed arm in man. *Journal of Neurophysiology* 69, 1443-1464.
- [7] Shadmehr R, Mussa-Ivaldi FA, Bizzi E (1993) Postural force fields of the human arm and their role in generating multijoint movements. *J Neurosci* 13:45-62
- [8] McIntyre J, Mussa-Ivaldi FA, Bizzi E (1996) The control of stable arm postures in the multi-joint arm. *Exp Brain Res* 110:62-73.
- [9] Gomi, H., Kawato, M., 1997. Human arm stiffness and equilibriumpoint trajectory during multijoint movement. *Biological Cybernetics* 76, 163-171.
- [10] Tsuji T, Morasso PG, Goto K, Ito K (1995) Hand impedance characteristics during maintained posture. *Biol Cybern* 72:475-485.
- [11] Dolan JM, Friedman MB, Nagurka ML (1993) Dynamic and loaded impedance components in the maintenance of human arm posture. *IEEE Trans Syst Man Cybern* 23:698-709.
- [12] E Burdet, R Osu, DW Franklin, TE Milner and M Kawato (2000). A Method for Measuring Hand Stiffness during Multi-joint Arm Movements. *Journal of Biomechanics* 33: 1705-09
- [13] Perreault EJ, Kirsch RF, Acosta AM (1999) Multiple-input, multiple-output system identification for the characterization of limb stiffness dynamics. *Biological Cybernetics* 80: 327-337.
- [14] Scott SH. Apparatus for measuring and perturbing shoulder and elbow joint positions and torques during reaching. *Journal of Neuroscience Methods*, Volume 89, Issue 2, 15 July 1999, Pages119-127.
- [15] Acosta AM, Kirsch RF, Perreault EJ. A robotic manipulator for the characterization of two-dimensional dynamic stiffness using stochastic displacement perturbations. *J Neurosci Methods* 2000;102:177-86.
- [16] Howard IS, Ingram JN, Wolpert DM. A modular planar robotic manipulandum with end-point torque control. *Journal of Neuroscience Methods*, Volume 181, Issue 2, 30 July 2009, Pages 199-211.
- [17] Burdet, E., Osu, R., 1999. Development of a new method for identifying muscle stiffness during human arm movements. Report 1-21, Kawato Dynamic Brain Project, ERATO, JST, Japan.
- [18] Robert L. Norton. *Cam Design and Manufacturing Handbook*. Industrial Press Copyright 2009, 592 pp. ISBN 0-8311-3367-2
- [19] Casadio M, Morasso P, Sanguineti V, Arrichiello V (2006) Braccio di Ferro: a new haptic workstation for neuromotor rehabilitation. *Technol Health Care* 14:123-142.